Vol. 104: 203–214, 2013
doi: 10.3354/dao02587

DISEASES OF AQUATIC ORGANISMS
Dis Aquat Org

Published June 13

Complete genome sequence and transcription profiles of the rock bream iridovirus RBIV-C1

Bao-Cun Zhang[1,2], Min Zhang[1], Bo-Guang Sun[1], Yong Fang[1,2], Zhi-Zhong Xiao[1], Li Sun[1,*]

[1]Institute of Oceanology, Chinese Academy of Sciences, Qingdao 266071, PR China
[2]Graduate University of the Chinese Academy of Sciences, Beijing 100049, PR China

ABSTRACT: The family *Iridoviridae* consists of 5 genera of double-stranded DNA viruses, including the genus *Megalocytivirus*, which contains species that are important fish pathogens. In a previous study, we isolated the first rock bream iridovirus from China (RBIV-C1) and identified it as a member of the genus *Megalocytivirus*. In this report, we determined the complete genomic sequence of RBIV-C1 and examined its *in vivo* expression profiles. The genome of RBIV-C1 is 112 333 bp in length, with a GC content of 55% and a coding density of 92%. RBIV-C1 contains 4584 simple sequence repeats, 89.8% of which are distributed among coding regions. A total of 119 potential open reading frames (ORFs) were identified in RBIV-C1, including the 26 core iridovirus genes; 41 ORFs encode proteins that are predicted to be associated with essential biological functions. RBIV-C1 exhibits the highest degree of sequence conservation and colinear arrangement of genes with orange-spotted grouper iridovirus (OSGIV) and rock bream iridovirus (RBIV). The pairwise nucleotide identities are 99.49% between RBIV-C1 and OSGIV and 98.69% between RBIV-C1 and RBIV. Compared to OSGIV, RBIV-C1 contains 11 insertions, 13 deletions, and 103 single nucleotide mutations. Whole-genome transcription analysis showed that following experimental infection of rock bream with RBIV-C1, all but 1 of the 119 ORFs were expressed at different time points and clustered into 3 hierarchical groups based on their expression patterns. These results provide new insights into the genetic nature and gene expression features of megalocytiviruses.

KEY WORDS: *Iridovirus* · *Megalocytivirus* · Comparative genome · *Oplegnathus fasciatus*

INTRODUCTION

Iridoviruses are a family of large, double-stranded DNA viruses that range from 120 to 200 nm in diameter. According to the Eighth Report of the International Committee on Taxonomy of Viruses, the family *Iridoviridae* is divided into 5 genera: *Iridovirus*, *Chloriridovirus*, *Lymphocystivirus*, *Ranavirus*, and *Megalocytivirus*, which differ in host range, particle size, and genetic characteristics (Chinchar et al. 2005, Williams et al. 2005). Viruses belonging to 3 genera, *Lymphocystivirus*, *Ranavirus*, and *Megalocytivirus*, are capable of infecting vertebrates including teleost fish. Of these viruses, megalocytiviruses are known to cause heavy economic losses in farmed fish, particularly in Asian countries such as China, Korea, and Japan (Kurita & Nakajima 2012). The host range of megalocytiviruses includes a variety of marine and freshwater fish species, notably rock bream, turbot, grouper, cichlids, red sea bream, gourami, and sea bass (Chou et al. 1998, Wang et al. 2003, Go et al. 2006, Whittington et al. 2010).

The complete genome sequences of at least 17 iridoviruses have been reported (Table 1). There are great variations with respect to genome size, GC content, and coding capacity between different genera of iridoviruses, and the genus *Megalocytivirus*, which includes ISKNV, RSIV, RBIV, OSGIV, TRBIV, and LYCIV, is divergent from all other genera. However, within the genus *Megalocytivirus*,

*Corresponding author. Email: lsun@qdio.ac.cn

Table 1. Iridoviruses from vertebrate and invertebrate hosts, for which the viral genomes have been completely sequenced

Virus	Abbreviation	GenBank accession no.	Reference
Lymphocystis disease virus type 1	LCDV-1	NC_001824	Tidona & Darai (1997)
Infectious spleen and kidney necrosis virus	ISKNV	NC_003494	He et al. (2001)
Chilo iridescent virus[a]	CIV	AF303741	Jakob et al. (2001)
Tiger frog virus	TFV	AF389451	He et al. (2002)
Red seabream iridovirus	RSIV	BD143114	Kurita et al. (2002)
Ambystoma tigrinum stebbensi virus	ATV	AY150217	Jancovich et al. (2003)
Rock bream iridovirus	RBIV	KC244182	Do et al. (2004)
Frog virus 3	FV-3	NC_005946	Tan et al. (2004)
Singapore grouper iridovirus	SGIV	NC_006549	Song et al. (2004)
Lymphocystis disease virus isolated in China	LCDV-C	NC_005902	Zhang et al. (2004)
Orange-spotted grouper iridovirus	OSGIV	AY894343	Lü et al. (2005)
Grouper iridovirus[b]	GIV	AY666015	Tsai et al. (2005)
Large yellow croaker iridovirus	LYCIV	AY779031	Ao & Chen (2006)
Invertebrate iridescent virus type 3	IIV-3	DQ643392	Delhon et al. (2006)
Soft-shelled turtle iridovirus[c]	STIV	EU627010	Huang et al. (2009)
Turbot reddish body iridovirus	TRBIV	GQ273492	Shi et al. (2010)
Rana grylio virus	RGV	JQ654586	Lei et al. (2012)

[a]Listed as species *Insect iridescent virus 6* (IIV-6) in the ICTV database (http://ictvonline.org)
[b]GIV is believed to be a related strain to SGIV
[c]STIV is believed to be a related strain to FV3

there exist high levels of sequence conservation and colinear arrangement of genes (Eaton et al. 2007). In general, different species of megalocytiviruses have comparable genome sizes (110–112 kb), GC content (53–55%), and numbers of open reading frames (ORFs; 115–124).

Zhang et al. (2012) reported the first rock bream iridovirus isolate from China, RBIV-C1, which had caused a severe epidemic outbreak. RBIV-C1 was classified as a megalocytivirus based on the sequences of conserved genes and histopathological symptoms of the infected fish. In the present study, we sequenced the complete genome of RBIV-C1 and analyzed its genetic features in comparison with other known megalocytiviruses. In addition, we also examined the transcription profiles of all predicted ORFs of RBIV-C1 during the course of infection in rock bream. Our results provide further understanding regarding the genetic nature and gene expression patterns of megalocytiviruses.

MATERIALS AND METHODS

Viral DNA preparation

Spleen and kidney from the moribund rock bream were homogenized in pre-cooled phosphate-buffered saline (PBS; pH 7.4), and the homogenate was centrifuged at 2500 × *g* (30 min at 4°C). The supernatant was filtered through a 0.2 µm membrane and stored at −80°C. Viral DNA preparation was performed as described by Shinmoto et al. (2009), and the obtained DNA was dissolved in TE buffer (10 mM Tris-HCl, 1 mM EDTA, pH 8.0).

PCR amplification and DNA sequencing

The complete genomic DNA of RBIV-C was sequenced using a PCR-based method. As RBIV-C showed high homology to RBIV and OSGIV, the primers were designed according to the DNA sequences of RBIV and OSGIV recovered from the GenBank database (accession nos. AY532606 and AY894343). The PCR products ranged from 1000 to 3000 bp in length, and the initial PCR products were designed to have at least 200 bp of overlapping sequence. PCR was conducted with a Biometra Tpersonal thermocycler in a volume of 20 µl containing 50 mM KCl, 20 mM Tris-HCl (pH 8.4), 1.5 mM $MgCl_2$, 0.1% Triton X-100, 100 pM of each primer, 0.2 mM of each dNTP, 1 U *Taq* DNA polymerase, and 100 ng template DNA. The PCR products were cloned into the T-A cloning vector pEASY-T1 (TransGen Biotech), and the recombinant plasmids were used for sequence determination with an ABI PRISM 3730 automated DNA sequencer in both directions with the universal primers of the plasmid (M13 Forward Primer and M13 Reverse Primer).

Sequence analysis

Genomic DNA composition, structure, and homologous regions were analyzed using DNASTAR. The ORFs and the encoded amino acid sequences were predicted using Genome Annotation Transfer Utility (http://athena.bioc.uvic.ca/help/tool-help/help-books/genome-annotation-transfer-utility-gatu-documentation/) and the National Center for Biotechnology Information (NCBI) ORF finder (www.ncbi.nlm.nih.gov/gorf/gorf.html). Protein database searches were conducted using BLASTP at the NCBI Web site (www.ncbi.nlm.nih.gov). Comparative genome analysis was performed with Clustal-X 2.0 (Larkin et al. 2007) and MAFFT (Katoh & Toh 2008). DNA dot matrix analysis was conducted using Java Dot Plot Alignments (Jdotter; Brodie et al. 2004).

In vivo transcriptional profile of RBIV-C1

Rock bream (average 14.6 g) were sourced from a fish farm in Shandong Province, China. RBIV-C1 was suspended in PBS to 1 $\times 10^6$ copies ml^{-1}. The fish were experimentally infected with RBIV-C1 by intraperitoneal injection of each fish with 100 µl RBIV-C1 suspension. At 0, 2, 5, 8, and 11 d post-infection (dpi), the spleens were removed from the sampled fish (4 fish per time point) and analyzed by quantitative real time reverse transcription-PCR (qRT-PCR). Total RNA was extracted from the tissues with the EZNA Total RNA Kit (Omega Bio-tek) and treated with RNase-free DNase I (MBI Fermentas). The quality of the RNA was examined by determining its 260/280 absorbance ratio using a NanoDrop 2000 (Thermo Scientific) and by gel electrophoresis. One microgram of total RNA was used for cDNA synthesis with ReverAid™ reverse transcriptase (MBI Fermentas) according to the manufacturer's instructions. qRT-PCR was carried out in an Eppendorf Mastercycler using the SYBR ExScript qRT-PCR Kit (Takara) as described previously (Zheng & Sun 2011). Melting curve analysis of amplification products was performed at the end of each PCR to confirm that only 1 PCR product was amplified and detected. The expression level of each gene was analyzed using the comparative threshold cycle method ($2^{-\Delta\Delta CT}$). The reaction was performed in triplicate, and the data are presented in terms of mRNA levels relative to that of β-actin and expressed as means ± SE.

Table 2. Summary of genomic information of 6 sequenced megalocytiviruses. RBIV-C1 sequence has the GenBank accession no. KC244182; other accession nos. and full virus names in Table 1. ORF: open reading frame

Virus	Geographic location	Genome size (bp)	G+C (%)	No. of ORFs
RBIV-C1	China	112333	53	119
OSGIV	China	112636	54	121
RBIV	Korea	112080	53	118
RSIV	Japan	112415	53	116
LYCIV	China	111760	54	–
TRBIV	China	110104	55	115
ISKNV	China	111362	55	124

RESULTS AND DISCUSSION

Characteristics of the RBIV-C1 genome

GC content and coding capacity

The complete genome of RBIV-C1 is similar in size to the genomes of RSIV, RBIV, OSGIV, LYCIV, TRBIV, and ISKNV (Table 2). Like most iridoviruses, the RBIV-C1 sequence is circularly permuted and was assembled into a circular form. RBIV-C1 has 55% G+C, which are distributed uniformly over the genome (Fig. 1). The GC content of RBIV-C1 is identical to that of TRBIV (55%), FV-3 (55%), and TFV (55%), comparable to those of ISKNV (54.8%), OSGIV (54%), ATV (54%), RBIV (53%), and SGIV (48.64%), and much higher than that of LCDV-C (27.25%) and LCDV-1 (29.1%). A total of 119 putative ORFs were identified in RBIV-C1, which include the 26 core genes of iridoviruses (Eaton et al. 2007). The number of ORFs is close to those of RBIV, TRBIV, OSGIV, and ISKNV (Table 2). Of the 119 ORFs of RBIV-C1, 48 (40.3%) are on the sense (R) DNA strand and 71 (59.7%) are on the antisense (L) strand. The sizes of the ORFs range from 120 to 3849 bp, and the corresponding encoded proteins range from 39 to 1282 residues in length (Fig. 1, see also Table S1 in the Supplement at www.int-res.com/articles/suppl/d104p203_supp.pdf). The total ORF length is 103 353 bp, which accounts for 92% of the entire genome. The percent coding density of RBIV-C1 is similar to OSGIV (91%), ISKNV (93%), and RBIV (86%).

Frequencies of simple sequence repeats (SSRs)

A genome-wide scan of RBIV-C1 identified a total of 4584 SSR tracts (Table 3), which are distributed evenly in the genome (Fig. 2). Of the 4584 SSRs, 4089,

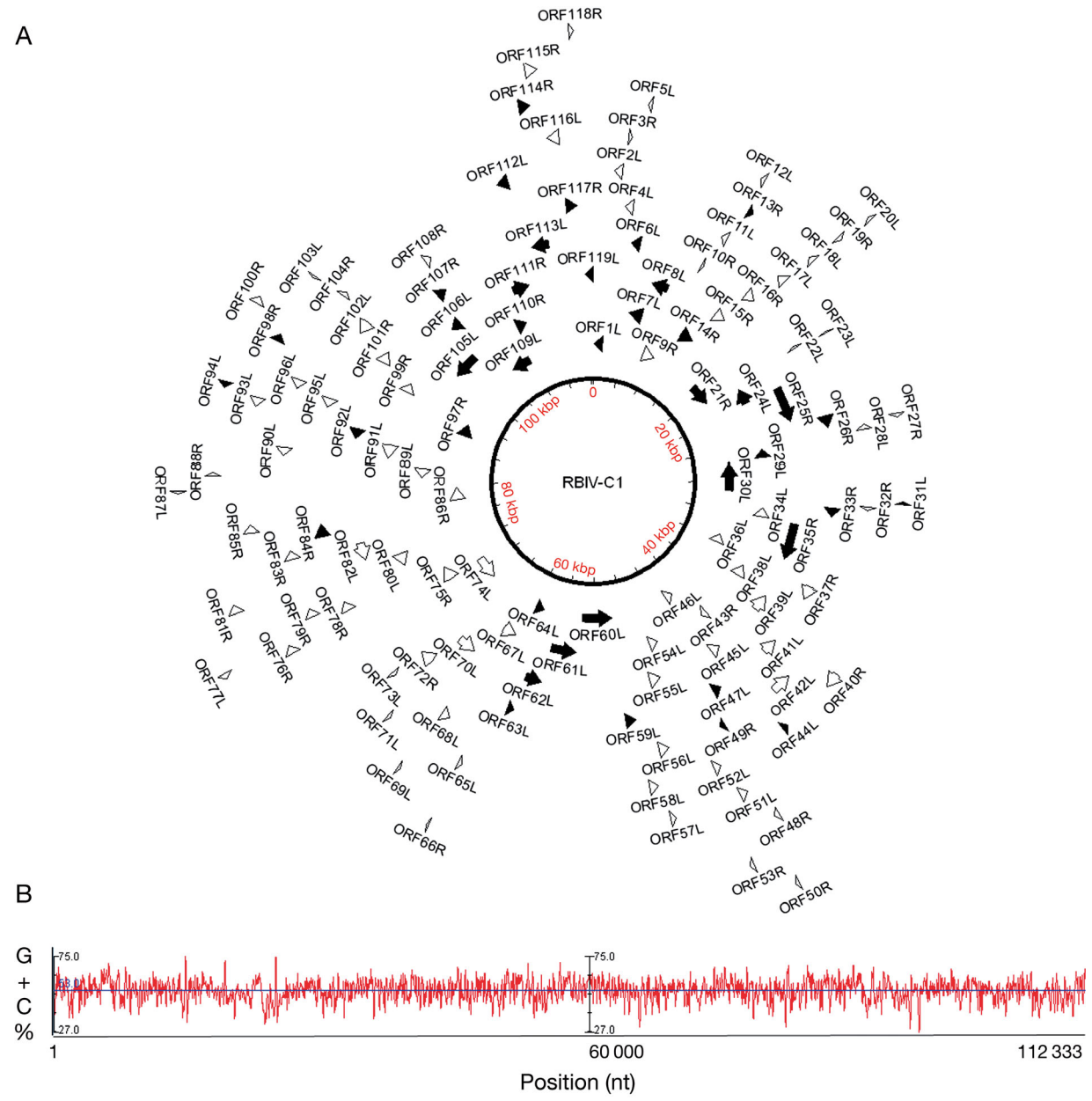

Fig. 1. Organization of the RBIV-C1 genome. (A) Predicted open reading frame (ORF) map. Arrows indicate the approximate size and transcription direction of the ORFs. White arrows represent ORFs with predicted functions, and black arrows represent ORFs with unknown function. (B) GC content

Table 3. Number of simple sequence repeats (SSR) in RBIV-C1

No. of SSRs per locus	Mono-nucleotide	Di-nucleotide	Tri-nucleotide	Tetra-nucleotide
3	3225	387	49	1
4	646	45	7	–
5	158	4	–	–
6	46	–	1	–
7	12	1	–	–
8	2	–	–	–

437, 57, and 1 are mono-, di-, tri-, and tetra-nucleotide, respectively. For mononucleotide SSRs, the number of repeats range between 3 and 8, although they are mostly 3 to 5. For di- and tri-nucleotide SSRs, 3 repeats occur most often, and the maximum repeats are 7 and 6, respectively. There is only 1 tetra-nucleotide SSR, which has 3 repeats. When the sequence of RBIV-C1 was screened for SSR locations relative to the ORFs, it was found that 89.8 and 10.2% of SSRs are distributed among coding and non-coding regions, respectively. Similarly, in bacteria, SSRs are lo-

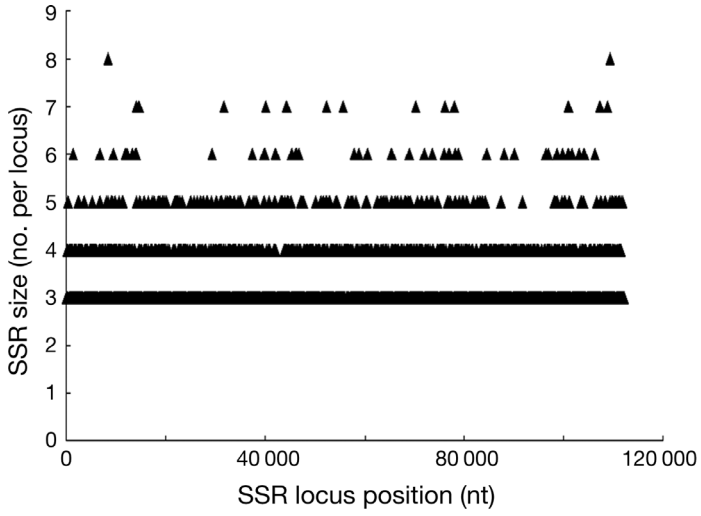

Fig. 2. Distribution and length of simple sequence repeats (SSRs) in RBIV-C1

cated in both ORFs and non-coding regions, and changes in SSRs can cause altered gene expression, which facilitates selection of bacterial populations that are better adapted to the host environment (Moxon et al. 2006, Power et al. 2009). The biological significance of viral SSRs is not clear. It remains to be investigated whether the non-coding SSRs in RBIV-C1 and other viruses have any regulatory effects on the expression of neighboring genes. In RBIV-C1, it is noteworthy that of the SSRs that are located in the coding regions, most occur in 4 ORFs, i.e. ORF60L, ORF30L, ORF35R, and ORF25R, which contain 149, 141, 135, and 130 SSRs, respectively.

Predicted functions of the ORF-encoded proteins

The ORFs of RBIV-C1 are in general highly conserved among known megalocytiviruses, in particular OSGIV and RBIV. Of the 119 ORFs identified in RBIV-C1, 117 have homologous counterparts in OSGIV and RBIV. The nucleotide sequence identities of the homologous ORFs are 96 to 100% between RBIV-C1 and OSGIV and 92 to 100% between RBIV-C1 and RBIV (Table S1). Among the ORFs, 86 are 100% identical between RBIV-C1 and OSGIV, and 37 ORFs are 100% identical between RBIV-C1 and RBIV (Table S1). Moreover, 41 ORFs encode proteins with predictable functions, including proteins associated with DNA replication, transcription, modification, virus structure, and host interaction (Table S1). Specifically, the ORFs involved in DNA replication and repair include 21R, 29L, 33R, 59L, 61L, 105L, and 107R, which encode a DNA polymerase, DNA repair protein RAD2, deoxyribonucleoside kinase, putative replication factor, SNF2 family helicase, D5 family NTPase, and proliferating cell nuclear antigen, respectively. These proteins play critical roles in viral DNA replication, repair, and recombination (Hamilton & Evans 2005, De Silva et al. 2007, Nash et al. 2007). ORF26R encodes the small chain of ribonucleotide reductase. This enzyme functions to reduce ribonucleotides into deoxyribonucleotides, the latter of which are used in the synthesis of DNA. Genes encoding the large and small subunits of ribonucleotide reductase are found in all iridoviruses except megalocytiviruses, in which only the small subunit is present (Kurita & Nakajima 2012). ORFs 14R, 24L, 44L, and 109L of RBIV-C1 encode a serine/threonine protein kinase catalytic domain, putative phosphatase, thiol oxidoreductase, and tyrosine kinase, respectively, which are likely to be involved in modification of viral and host proteins. ORFs 30L, 31L, 35R, 62L, and 84R encode the largest subunit of the DNA-dependent RNA polymerase, transcription elongation factor SII, RNA polymerase beta subunit, mRNA capping enzyme, and ribonuclease III, respectively. These proteins are 94 to 100% identical to their respective counterparts in OSGIV and RBIV, which are involved in viral RNA processing, transcription elongation, and regulation (Ito et al. 2006, Kim et al. 2007). Putative viral structural proteins include transmembrane amino acid transporter protein (ORF1L), proteins with transmembrane domains (ORF5L, ORF51L, ORF52L, and ORF93L), major capsid protein (ORF7L), and myristylated membrane proteins (ORF8L, ORF55L, and ORF56L). In a proteomic study of SGIV, the myristylated membrane proteins were identified as envelope proteins, and the protein equivalent to ORF8L was found to bind a membrane protein of the host grouper (Zhou et al. 2011). In RBIV-C1, putative virus–host interaction proteins include RING-finger-containing ubiquitin ligase (ORF13R, ORF63L, ORF64L), laminin-type epidermal growth factor-like protein (ORF25R), vascular endothelial growth factor-like protein (ORF49R), RING-finger domain-containing protein (ORF94L and ORF114R), ankyrin repeat-containing protein (ORF97R, ORF113L, and ORF119L), suppressor of cytokine signaling protein (ORF98R), and tumor necrosis factor receptor-associated factor (ORF106L). These proteins are highly conserved among iridoviruses. In ISKNV, the RING-finger domain-containing proteins encoded by ORF12, ORF65, ORF66, and ORF111

(equivalent to RBIV-C1 ORF13R, ORF63L, and ORF64L) possess ubiquitin ligase activity in a manner that depends on the RING motif (Xie et al. 2007), and that ORF48R (equivalent to RBIV-C1 ORF49R) is able to induce vascular permeability in zebrafish and cause pericardial edema of zebrafish embryos (Wang et al. 2008).

Genomic comparison between RBIV-C1 and other megalocytiviruses

Global pairwise alignment

Sequence alignment showed that the overall genome sequence of RBIV-C1 resembles most closely those of OSGIV and RBIV, with the pairwise nucleotide identities being 99.5% between RBIV-C1 and OSGIV and 98.7% between RBIV-C1 and RBIV. To further examine the global sequence conservation between RBIV-C1 and OSGIV and RBIV as well as 2 other fully sequenced megalocytiviruses, i.e. TRBIV and ISKNV, a nucleotide-to-nucleotide comparison was conducted. The resulting dot plots revealed the highest levels of sequence colinearity between RBIV-C1 and OSGIV and RBIV (Fig. 3), suggesting the existence of high degrees of sequence conservation among these viruses. Alignment of RBIV-C1 with TRBIV and ISKNV showed large gaps (over 100 bp) that disrupt the colinearities of the aligned sequences, suggesting that compared to OSGIV and RBIV, TRBIV and ISKNV exhibit lesser degrees of sequence identities with RBIV-C1.

Single nucleotide polymorphisms (SNPs)

Since RBIV-C1 is most closely related to OSGIV and RBIV, we compared RBIV-C1 with these 2 viruses in more detail. A survey of SNPs indicated that when OSGIV was used as a reference, RBIV-C1 exhibits 103 SNPs, 89 and 14 of which are located in the coding and non-coding regions, respectively (Fig. 4, Table 4). Of the 89 coding-region SNPs, 28 are synonymous mutations and 61 are non-synonymous mutations, 12 of the latter being clustered in ORF35. Compared to RBIV, RBIV-C1 contains 485 SNPs, 449 of which are located in the coding region. Of the 449 coding-region SNPs, 262 are non-synonymous mutations and are distributed widely in different ORFs. In contrast to OSGIV and RBIV, when RSIV was used as a reference, the SNPs in RBIV-C1 increased drastically to 3145.

Insertions/deletions

With OSGIV as a reference, 11 insertions and 13 deletions were identified in RBIV-C1, of which 9 insertions and 10 deletions are in the coding regions (Fig. 5A,B, Table 4). Compared to RBIV, RBIV-C1 contains 51 insertions and 44 deletions, with 34 insertions and 40 deletions located in the coding regions (Fig. 5C,D, Table 4). Of the insertions/deletions between RBIV-C1 and OSGIV, 4 are over 60 bp in size and distributed in ORF27R, ORF95L, and ORF111R (Fig. 6). Seven >60 bp insertions/deletions were found between RBIV-C1 and RBIV, which are located in ORF19R, ORF25R, ORF27R, ORF70L, ORF111R, and ORF119L (Fig. 6). Some of the insertions/deletions cause frame shift and consequently alter the sequence of the encoded proteins. For instance, compared to the ORF35L of OSGIV, the counterpart ORF of RBIV-C1, i.e. ORF32L, has 2 tandem adenine insertions, which result in an encoded protein with 13 more residues. In addition, comparative genomic analysis revealed that ORF60L of RBIV-C1, which encodes a putative DNA-binding protein, is absent in OSGIV. The occurrence of ORF60L in RBIV-C1 is due to deletion of a cytosine at the position of 54 921 bp of RBIV-C1. It will be interesting to examine, e.g. via mutational analysis, whether these differences in ORF and proteins are associated with host-specific infection.

In vivo transcription profiles of the 119 predicted ORFs of RBIV-C1

To examine the expression patterns of the predicted RBIV-C1 genes represented by the 119 ORFs, rock bream were infected with RBIV-C1, and the

Table 4. Single nucleotide polymorphisms (SNPs) and insertions/deletions of RBIV-C1 in comparison with OSGIV and RBIV

	OSGIV		RBIV	
SNPs	103		485	
Non-coding	14		36	
Coding	89		449	
Synonymous	28		187	
Non-synonymous	61		262	
Insertions/ deletions	Coding region	Intergenic region	Coding region	Intergenic region
Insertions	9	2	34	17
Deletions	10	3	40	4
Total	19	5	74	21

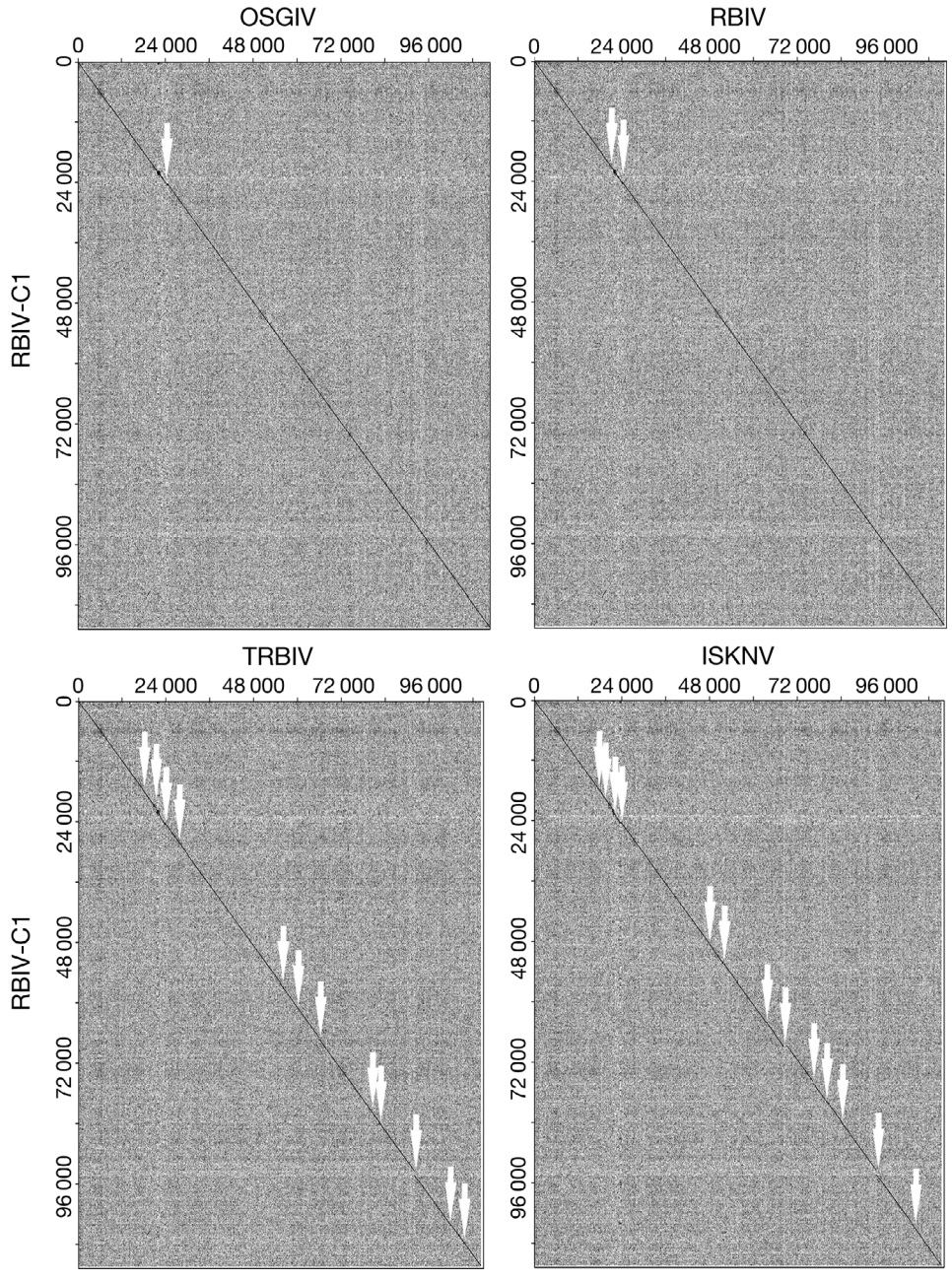

Fig. 3. Alignment of the genomic sequence of RBIV-C1 with those of OSGIV, RBIV, TRBIV, and ISKNV by dot matrix plots. In each case, the *y*-axis represents RBIV-C1. Solid lines indicate colinearity, and white arrows indicate >100 bp gaps between the aligned genomes

mRNA levels of the 119 ORFs in spleen were determined by qRT-PCR at 5 time points, i.e. 0, 2, 5, 8, and 11 dpi, which represent roughly the early, middle, and late infection stages. At the early infection time (2 dpi), fish behaved normally and exhibited no pathological signs; at the middle infection stage (5 to 8 dpi), clinical symptoms were observed in some fish; at the late infection stage (11 dpi), mortality began to occur. The results of qRT-PCR showed that at 2 dpi, 69 (58%) ORFs were found to be in expression, with high levels (69- to 109-fold) of expression observed with ORF66R, ORF107R, ORF119L, and ORF118R. In a previous microarray analysis of gene transcription of RSIV during *in vitro* infection, Lua et al. (2005) observed that 6.5% of total viral ORFs commenced expression at 3 h post-infection, and that by 48 h post-infection, 95.7% of the ORFs were expressed. Likewise, in our study, we found that as the infection

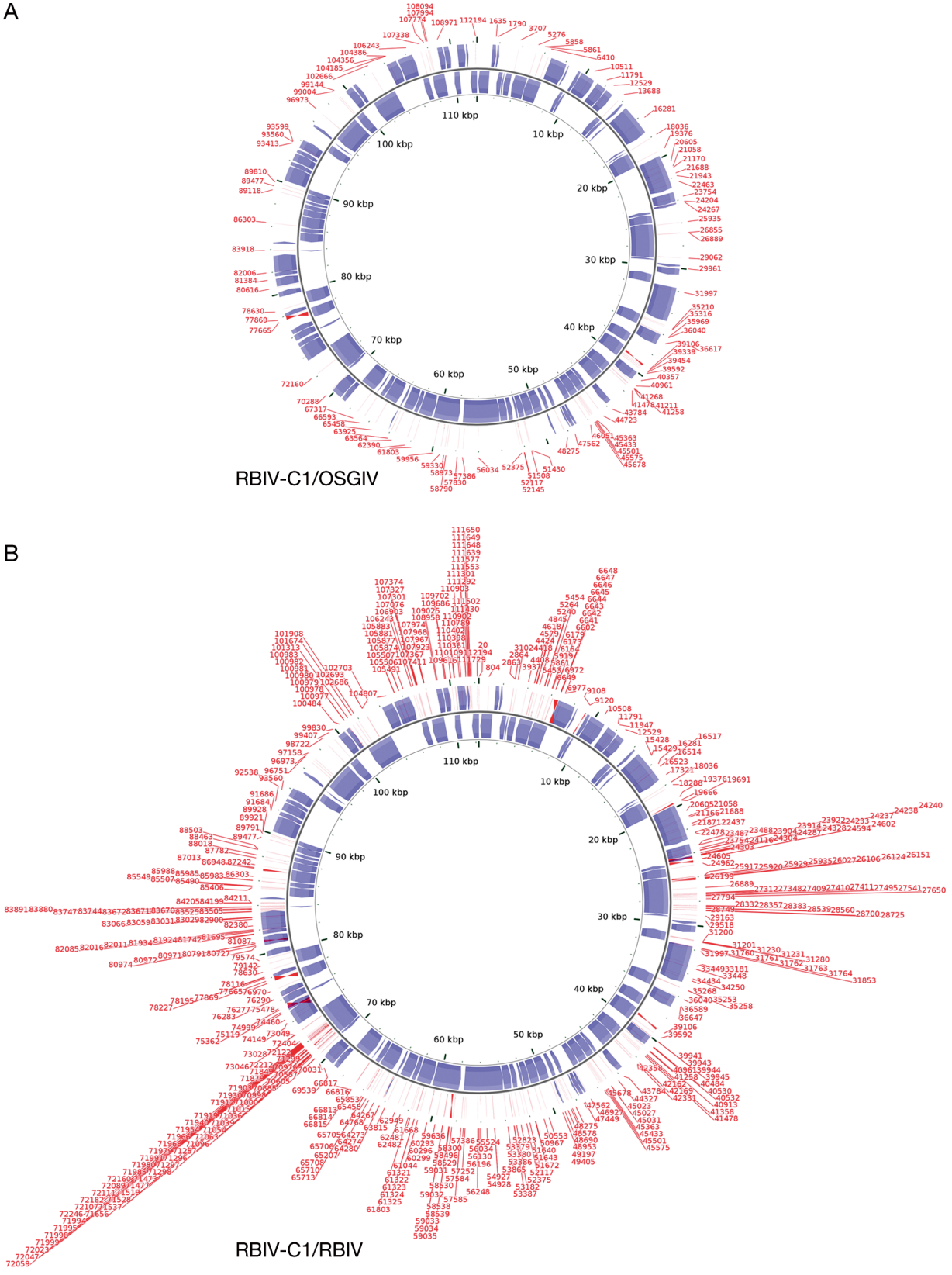

Fig. 4. Single nucleotide mutations (SNPs) of RBIV-C1 in comparison with (A) OSGIV and (B) RBIV. Red lines outside the map indicate the positions of the SNPs, and the blue color represents coding regions

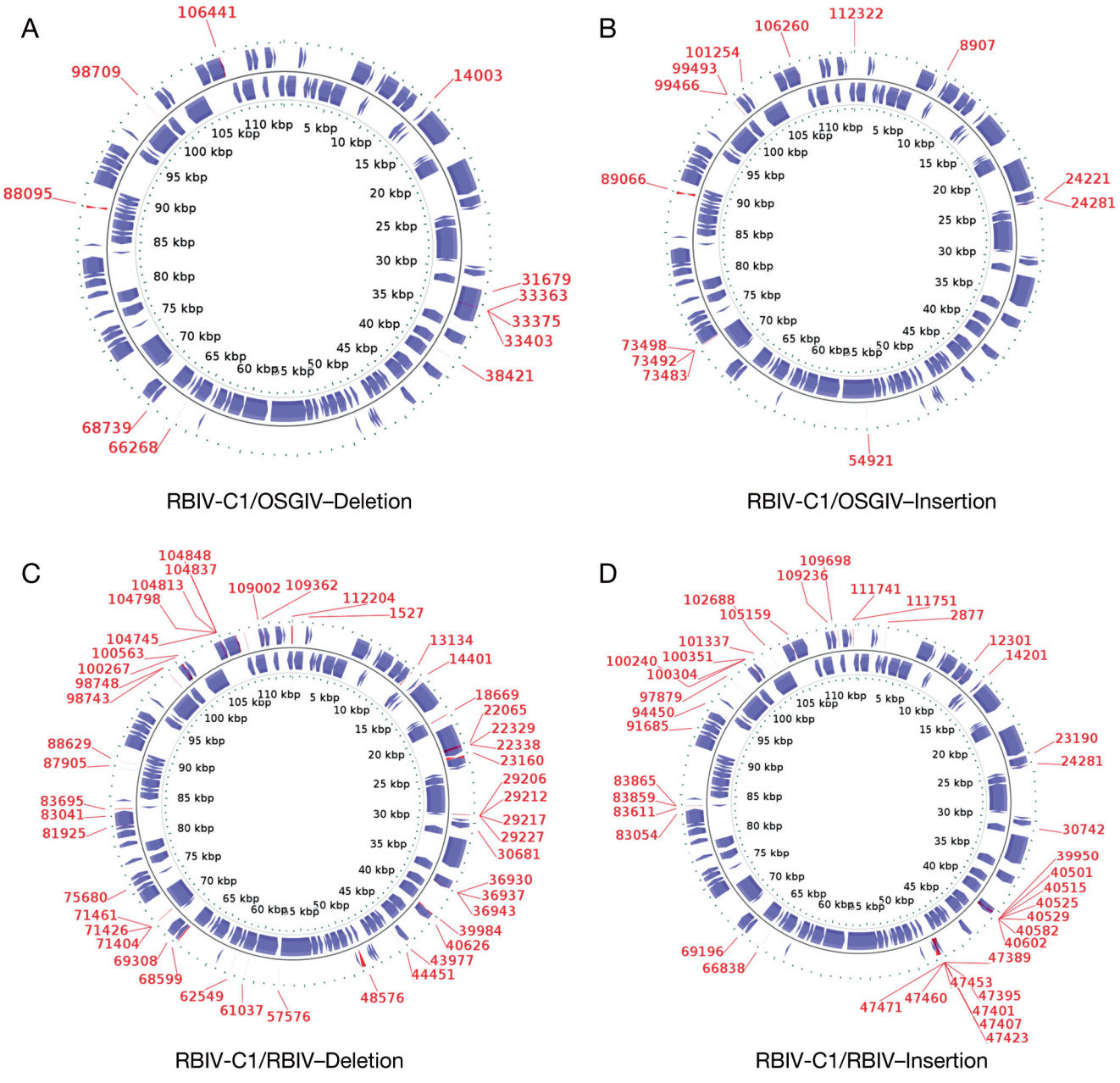

Fig. 5. Deletions/insertions between (A,B) RBIV-C1 and OSGIV and (C,D) RBIV. Numbers indicate the beginning positions of deletions or insertions, and the blue color represents coding regions

progressed, the number of expressed ORFs increased rapidly and reached 117 (98%) at 5 and 8 dpi. At these 2 time points, the only 2 ORFs that remained comparable in expression level to 0 dpi were ORF26R and ORF112L. At 11 dpi, expression of all ORFs except for ORF112 was detected. ORF112 was the only ORF whose expression was not detected at all of the examined time points. A previous study of SGIV revealed that 90 to 94% viral genes were significantly expressed in the early infection stage between 1 and 4 dpi and reached peak expression at 4 dpi, and that the expression levels of most genes began to decrease after 5 dpi (Teng et al. 2008). In our study, 18 (15%) and 100 (84%) ORFs reached maximum expression at 8 and 11 dpi, respectively. Compared to other ORFs, ORF119, ORF66, ORF118, ORF52, and ORF56 have the highest expression levels at all time points.

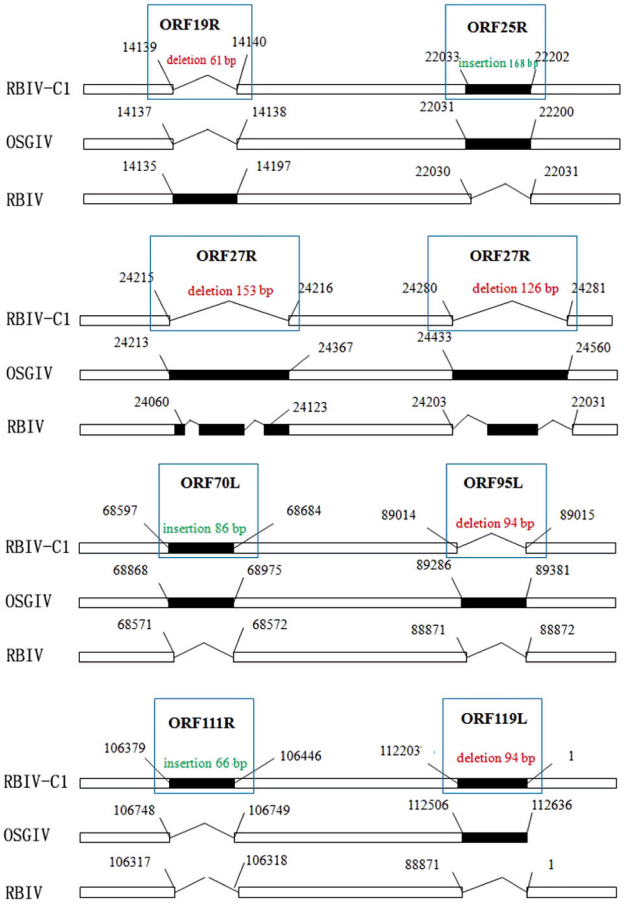

Fig. 6. Schematic representation of the major insertions/deletions between RBIV-C1 and OSGIV and RBIV. Numbers indicate positions of the insertions/deletions, white bars represent genome fragments, black bars indicate insertions, and thin lines indicate deletions

Hierarchical clustering, in which the expression of each gene at every time point was compared and classified according to similarities in expression trends and in the change rate of expression levels, was applied to analyze the expression patterns of the 119 ORFs. The results are illustrated in Fig. 7. The first level of classification was based on expression trends, which showed that the 119 genes were classified into 3 groups. The first group consists of 94 genes, which expressed at increased levels as the infection progressed; the second group consists of 19

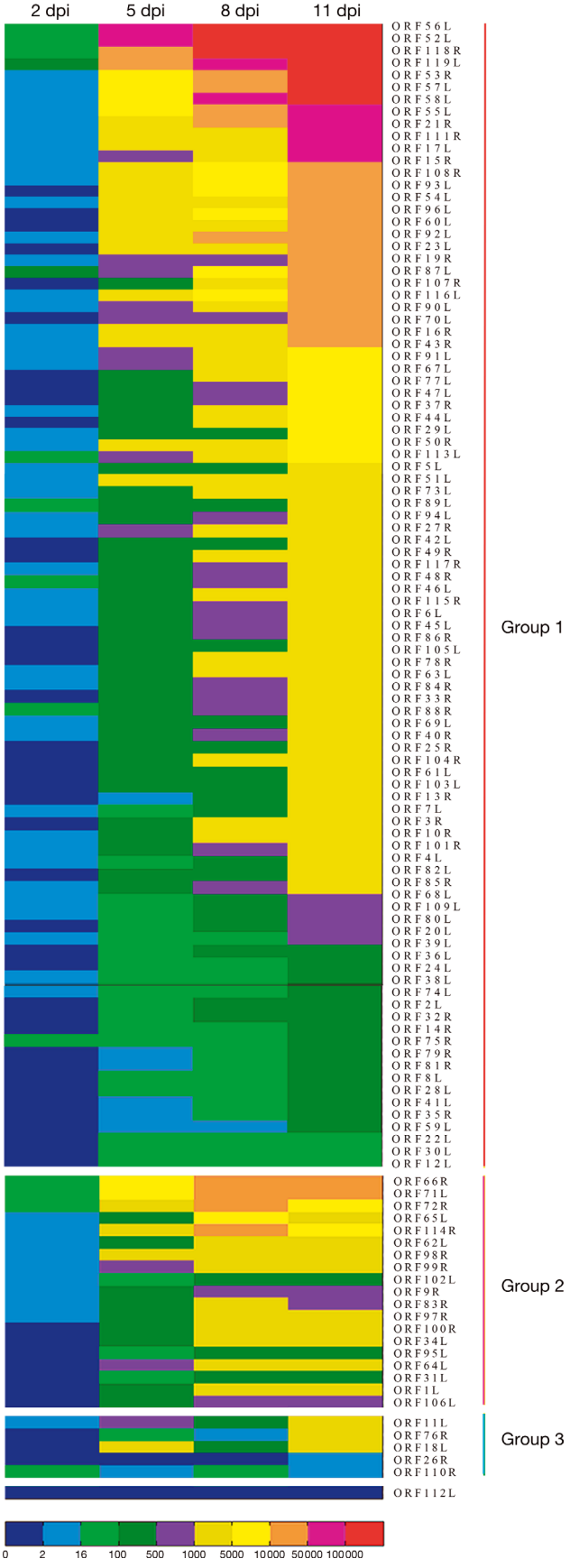

Fig. 7. Temporal expression patterns (days post-infection, dpi) of RBIV-C1 open reading frames shown in a colored mosaic matrix. The 10 different color bars stand for expression levels of 0- to 2-fold, 2- to 16-fold, 16- to 100-fold, … , and >100000-fold, respectively

genes (ORF1L, ORF9R, ORF31L, ORF34L, ORF62L, ORF64L, ORF65L, ORF66R, ORF71L, ORF72R, ORF-83R, ORF95L, ORF97R, ORF98R, ORF99R, ORF100R, ORF102L, ORF106L, and ORF114R), whose expression increased at first and then decreased with the process of infection. The third group contains 5 genes (ORFs 11L, 18L, 26R, 76R, and 110R), which displayed diphasic expression patterns. Within each group, a second level of classification was applied based on the rate at which the expression level changed. For example, within the first group of the 94 genes that exhibited increased expression throughout the course of infection, 22 genes expressed at relative slowly increasing rates, 44 genes expressed at moderately increasing rates, and 28 genes expressed at dramatically increasing rates. Overall, the qRT-PCR data indicate that the majority of the predicted genes exhibited enhanced expression from early to late infection stages, which suggests that the virus had experienced replication, transcription, translation, and viral particle assembly in the infected host during the examined time course.

CONCLUSION

The results of this study demonstrate that RBIV-C1 resembles known megalocytiviruses in general genomic organization, GC content, coding capacity, and conserved essential genes. RBIV-C1 is most closely related to OSGIV and shares more than 99% sequence identity with the latter, suggesting that RBIV-C1 and OSGIV are likely 2 variant strains of the same species. These results indicate a high level of homology between different *Megalocytivirus* isolates, in particular among those identified in China, which suggests a possible genetic origin from the same evolutionary lineage. Since the Chinese isolates were from different fish species, it will be interesting for future studies to compare their host ranges. Compared to OSGIV and RBIV, RBIV-C1 possesses distinct sequence features as reflected in the characteristic SNPs, deletions, and insertions, which may serve as diagnostic markers for the identification of different strains. Whole-genome transcription analysis showed that of the 119 ORFs contained in RBIV-C1, 118 were expressed during *in vivo* infection and, based on their expression patterns, grouped roughly into 3 hierarchical clusters. These results add new information to the genetic nature of megalocytiviruses and provide a basis for future study of gene expression and regulation in megalocytiviruses.

Acknowledgements. This work was supported by grants from the National Basic Research Program of China (2012CB114406), the 863 High Technology Project of the Ministry of Science and Technology (2012AA10A413-1), the Knowledge Innovation Program of the Chinese Academy of Sciences (KZCX2-EW-Q213 and KZCX2-EW-Q213), and the Taishan Scholar Program of Shandong Province.

LITERATURE CITED

Ao J, Chen X (2006) Identification and characterization of a novel gene encoding an RGD-containing protein in large yellow croaker iridovirus. Virology 355:213–222

Brodie R, Roper RL, Upton C (2004) JDotter: a Java interface to multiple dotplots generated by dotter. Bioinformatics 20:279–281

Chinchar VG, Essbauer JG, He JG, Hyatt A, Miyazaki T, Seligy V, Williams T (2005) Family *Iridoviridae*. In: Fauquet CM, Mayo MA, Maniloff J, Desselberger U, Ball LA (eds) Virus taxonomy. Eighth Report of the International Committee on Taxonomy of Viruses. Academic Press, San Diego, CA, p 145–162

Chou HY, Hsu CC, Peng TY (1998) Isolation and characterization of a pathogenic iridovirus from cultured grouper (*Epinephelus* sp.) in Taiwan. Fish Pathol 33:201–206

De Silva FS, Lewis W, Berglund P, Koonin EV, Moss B (2007) Poxvirus DNA primase. Proc Natl Acad Sci USA 104: 18724–18729

Delhon G, Tulman ER, Afonso CL, Lu ZQ and others (2006) Genome of invertebrate iridescent virus type 3 (mosquito iridescent virus). J Virol 80:8439–8449

Do JW, Moon CH, Kim HJ, Ko MS and others (2004) Complete genomic DNA sequence of rock bream iridovirus. Virology 325:351–363

Eaton HE, Metcalf J, Penny E, Tcherepanov V, Upton C, Brunetti CR (2007) Comparative genomic analysis of the family *Iridoviridae*: re-annotating and defining the core set of iridovirus genes. Virol J 4:11

Go J, Lancaster M, Deece K, Dhungyel O, Whittington R (2006) The molecular epidemiology of iridovirus in Murray cod (*Maccullochella peehi peehi*) and dwarf gourami (*Colisa lalia*) from distant biogeographical regions suggests a link between trade in ornamental fish and emerging iridoviral diseases. Mol Cell Probes 20:212–222

Hamilton MD, Evans DH (2005) Enzymatic processing of replication and recombination intermediates by the vaccinia virus DNA polymerase. Nucleic Acids Res 33: 2259–2268

He JG, Deng M, Weng SP, Li Z and others (2001) Complete genome analysis of the mandarin fish infectious spleen and kidney necrosis iridovirus. Virology 291:126–139

He JG, Lu L, Deng M, He HH and others (2002) Sequence analysis of the complete genome of an iridovirus isolated from the tiger frog. Virology 292:185–197

Huang Y, Huang X, Liu H, Gong J and others (2009) Complete sequence determination of a novel reptile iridovirus isolated from soft-shelled turtle and evolutionary analysis of *Iridoviridae*. BMC Genomics 10:224

Ito T, Arimitsu N, Takeuchi M, Kawamura N and others (2006) Transcription elongation factor S-II is required for definitive hematopoiesis. Mol Cell Biol 26:3194–3203

Jakob NJ, Muller K, Bahr U, Dara G (2001) Analysis of the first complete DNA sequence of an invertebrate iri-

dovirus: coding strategy of the genome of Chilo iridescent virus. Virology 286:182–196

Jancovich JK, Mao JH, Chinchar VG, Wyatt C and others (2003) Genomic sequence of a ranavirus (family *Iridoviridae*) associated with salamander mortalities in North America. Virology 316:90–103

Katoh K, Toh H (2008) Recent developments in the MAFFT multiple sequence alignment program. Brief Bioinform 9: 286–298

Kim B, Nesvizhskii AI, Rani PG, Hahn S, Aebersold R, Ranish JA (2007) The transcription elongation factor TFIIS is a component of RNA polymerase II preinitiation complexes. Proc Natl Acad Sci USA 104:16068–16073

Kurita J, Nakajima K (2012) Megalocytiviruses. Viruses 4: 521–538

Kurita J, Nakajima K, Hirono I, Aoki T (2002) Complete genome sequencing of red sea bream iridovirus (RSIV). Fish Sci 68:1113–1115

Larkin MA, Blackshields G, Brown NP, Chenna R and others (2007) Clustal W and Clustal X version 2.0. Bioinformatics 23:2947–2948

Lei XY, Ou T, Zhu RL, Zhang QY (2012) Sequencing and analysis of the complete genome of *Rana grylio* virus (RGV). Arch Virol 157:1559–1564

Lü L, Zhou SY, Chen C, Weng SP, Chan SM, He JG (2005) Complete genome sequence analysis of an iridovirus isolated from the orange-spotted grouper, *Epinephelus coioides.* Virology 339:81–100

Lua DT, Yasuike M, Hirono I, Aoki T (2005) Transcription program of red sea bream iridovirus as revealed by DNA microarrays. J Virol 79:15151–15164

Moxon R, Bayliss C, Hood D (2006) Bacterial contingency loci: the role of simple sequence DNA repeats in bacterial adaptation. Annu Rev Genet 40:307–333

Nash K, Chen WJ, McDonald WF, Zhou XH, Muzyczka N (2007) Purification of host cell enzymes involved in adeno-associated virus DNA replication. J Virol 81: 5777–5787

Power PM, Sweetman WA, Gallacher NJ, Woodhall MR, Kumar GA, Moxon ER, Hood DW (2009) Simple sequence repeats in *Haemophilus influenzae.* Infect Genet Evol 9:216–228

Shi CY, Jia KT, Yang B, Huang J (2010) Complete genome sequence of a Megalocytivirus (family *Iridoviridae*) associated with turbot mortality in China. Virol J 7:159

Shinmoto H, Taniguchi K, Ikawa T, Kawai K, Oshima S (2009) Phenotypic diversity of infectious red sea bream iridovirus isolates from cultured fish in Japan. Appl Environ Microbiol 75:3535–3541

Song WJ, Oin QW, Qiu J, Huang CH, Wang F, Hew CL (2004) Functional genomics analysis of Singapore grouper iridovirus: complete sequence determination and proteomic analysis. J Virol 78:12576–12590

Tan WGH, Barkman TJ, Chinchar VG, Essani K (2004) Comparative genomic analyses of frog virus 3, type species of the genus *Ranavirus* (family *Iridoviridae*). Virology 323: 70–84

Teng Y, Hou ZW, Gong J, Liu H and others (2008) Whole-genome transcriptional profiles of a novel marine fish iridovirus, Singapore grouper iridovirus (SGIV) in virus-infected grouper spleen cell cultures and in orange-spotted grouper, *Epinephulus coioides.* Virology 377: 39–48

Tidona CA, Darai G (1997) The complete DNA sequence of lymphocystis disease virus. Virology 230:207–216

Tsai CT, Ting JW, Wu MH, Wu MF, Guo IC, Chang CY (2005) Complete genome sequence of the grouper iridovirus and comparison of genomic organization with those of other iridoviruses. J Virol 79:2010–2023

Wang CS, Shih HH, Ku CC, Chen SN (2003) Studies on epizootic iridovirus infection among red sea bream, *Pagrus major* (Temminck & Schlegel), cultured in Taiwan. J Fish Dis 26:127–133

Wang ZL, Xu XP, He BL, Weng SP and others (2008) Infectious spleen and kidney necrosis virus ORF48R functions as a new viral vascular endothelial growth factor. J Virol 82:4371–4383

Whittington RJ, Becker JA, Dennis MM (2010) Iridovirus infections in finfish — critical review with emphasis on ranaviruses. J Fish Dis 33:95–122

Williams T, Barbosa-Solomieu V, Chinchar VG (2005) A decade of advances in iridovirus research. Adv Virus Res 65:173–248

Xie J, Zhu J, Yang H, Weng S and others (2007) RING finger proteins of infectious spleen and kidney necrosis virus (ISKNV) function as ubiquitin ligase enzymes. Virus Res 123:170–177

Zhang M, Xiao ZZ, Hu YH, Sun L (2012) Characterization of a megalocytivirus from cultured rock bream, *Oplegnathus fasciatus* (Temminck & Schlege), in China. Aquacult Res 43:556–564

Zhang QY, Xiao F, Xie H, Li ZQ, Gui HF (2004) Complete genome sequence of lymphocystis disease virus isolated from China. J Virol 78:6982–6994

Zheng WJ, Sun L (2011) Evaluation of housekeeping genes as references for quantitative real time RT-PCR analysis of gene expression in Japanese flounder (*Paralichthys olivaceus*). Fish Shellfish Immunol 30:638–645

Zhou S, Wan QJ, Huang YH, Huang XH and others (2011) Proteomic analysis of Singapore grouper iridovirus envelope proteins and characterization of a novel envelope protein VP088. Proteomics 11:2236–2248

Editorial responsibility: Mark Crane, Geelong, Victoria, Australia

Submitted: December 3, 2012; Accepted: February 11, 2013
Proofs received from author(s): May 9, 2013